International Journal of GEOMATE, Aug., 2021, Vol.21, Issue 84, pp.121-128
ISSN: 2186-2982 (P), 2186-2990 (O), Japan, DOI: https://doi.org/10.21660/2021.84.j2170
Geotechnique, Construction Materials and Environment

SHAFT RESISTANCE OF PILES CLOSE TO BACKFILLED SAND COLUMNS

* Hiroshi Nagai[1]

[1] College of Design and Manufacturing Technology, Muroran Institute of Technology, Japan

*Corresponding Author, Received: 12 April 2021, Revised: 21 May 2021, Accepted: 12 June 2021

ABSTRACT: In most reconstructions, existing old pile foundations are removed to construct new foundations. After removing the existing pile, the hole is backfilled, but there are issues such as different conditions from the surrounding ground. We report axial compressive loading model tests to investigate the shaft resistance of piles close to backfilled sand. In these model tests, the sandy ground is prepared in a chamber and a backfilling process is simulated, with varied backfilled sand density. The tests reveal that the maximum shaft resistance of the pile depends on the density of the backfilled sand. A numerical finite element method analysis is also performed to examine shear failure in the soil near the pile, which contributes to the shaft resistance mechanism of the pile. When the conditions of the backfilled sand are different from those of the soil, the shear stress of the soil near the pile is affected in both the backfilled sand area and the soil opposite the backfilled sand, and the shape and thickness of the shear band that occurs near the pile changes.

Keywords: New pile, Backfilled soil, Single pile, Pile shaft resistance, Loading test, Finite element method

1. INTRODUCTION

Reusing existing foundations for a structure reconstruction is effective both economically and environmentally, as it can shorten the construction period, reduce costs, and reduce construction waste and the environmental load associated with construction. The durability of existing foundation members buried underground and the bearing capacity of existing piles have been investigated and data has been accumulated through surveys and research, and guides and manuals on the reuse of existing old foundations have been published [1-2]. A case study on the reuse of existing foundations including existing old piles in a new structure and bridge has also been reported [3-9].

However, in most reconstructions, existing old pile foundations are removed to construct new foundations. After removing the old piles, the remaining holes should, in principle, be backfilled to match the conditions of the surrounding ground, and for this the nonuniformity of the backfilled material and differences from the surrounding ground are an issue. For a high-rise building, since long piles with large diameters are used, the scale of backfilling columns after removing old piles becomes large. Furthermore, when new piles are inserted close to the backfilled material after the removal of existing piles, the bearing performance of the new piles, especially the shaft resistance, may be affected.

There are many previous studies on the shaft resistance of piles. The previous studies include investigations of the friction between the pile material and soil [10-12], the peak strength and dilation of sand–steel interfaces [13], a numerical approach to estimate shaft friction considering dilatancy and strain softening of piles in sand deposits [14], a numerical simulation considering the cross-anisotropy and intermediate principal stress for evaluating shaft resistance of piles installed in sand [15], and a numerical parametric study using distinct element modelling (DEM) to investigate shearing mechanisms at pile–soil interfaces [16]. However, no prior research has considered a case where the backfilled material approaches part of the ground around the new pile.

In this study, we simulated the backfilling process with model sand and conducted an axial compressive loading test of a new pile close to the backfilled sand. We changed the density of the backfilled sand and focused on the shaft resistance of the pile. We also performed a numerical analysis using the finite element method (FEM) to examine stress and shear failure in the soil near the pile, which contributes to the shaft resistance mechanism of the pile.

2. AXIAL COMPRESSIVE LOADING TEST OF PILE CLOSE TO BACKFILLED SAND

2.1 Outline of Experiment

Fig. 1 shows the experimental construction process and an outline of the experimental apparatus is shown in Fig. 2. The model soil is dry Tohoku quartz sand number 6, shown in Table 1. The model soil has a relative density, D_r, of 60% and is prepared by air pluviation in a cylindrical chamber. A model pile and a crescent-shaped

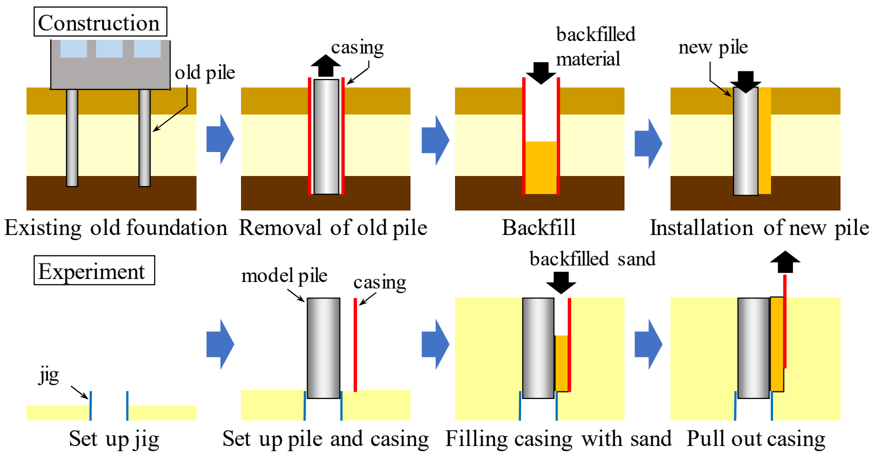

Fig. 1 Experimental construction process

casing, according to the shape of the pile, made from a copper plate with a thickness of 0.3 mm are set up. For the backfilled sand, sand of a predetermined relative density is deposited in the casing by controlling the falling height of the sand and the use of a net, as shown in Fig. 3, using the sand supply device of Fig. 4. The pile is made into a test specimen in which half the diameter of the pile overlaps with the backfilled sand. Earth pressure cells are placed at two depths in the soil at the positions shown in Fig. 5.

Table 1 Physical properties of Tohoku quartz sand

maximum density, ρ_{dmax} (g/cm^3)	1.712
minimum density, ρ_{dmin} (g/cm^3)	1.397
mean grain size, D_{50} (mm)	0.32
coefficient of uniformity, U_c	2.3
coefficient of curvature, U_c'	1.3

The model pile is a closed-end aluminum pipe that has a diameter, d, of 30 mm and thickness of 2 mm. The outer surface of the pile is roughened by a thermal sprayed coating (surface roughness of pile: R_{max} = 200 μm). Strain gauges are attached inside the pile to measure the stress on the G1 to G5 cross-sections shown in Fig. 6. The pile is embedded 300 mm in the center of the chamber, and the tip is inserted into a cylindrical jig so that the pile exhibits no tip resistance. The jig, shown in Fig. 7, is designed to prevent sand from entering and reducing friction with the pile.

After the test specimen is prepared, a restraining pressure due to water pressure, with a vertical pressure of σ_{v0} = 200 kPa and horizontal pressure of σ_{h0} = 100 kPa, is applied to the soil through a rubber membrane. An axial compressive loading test is carried out in which a load is applied to the pile head using hydraulic pressure. During the loading test, the pile head load, pile head displacement, earth pressure, and axial strain of the pile are measured by a load cell, a displacement transducer, earth pressure cells, and strain gauges,

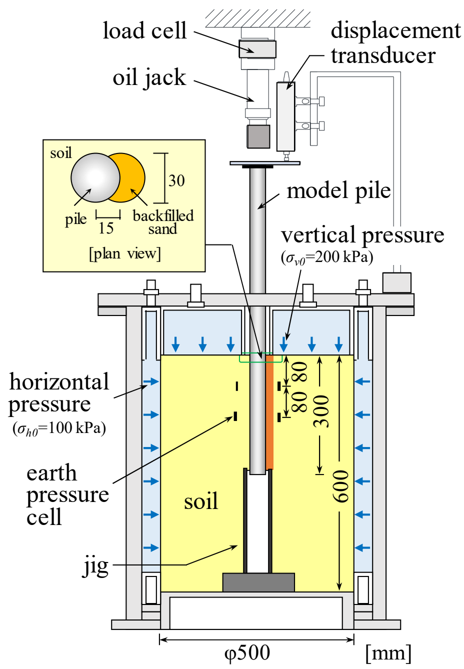

Fig. 2 Set up experiment device

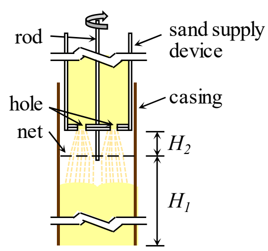

Fig. 3 Method for backfilling sand into the casing

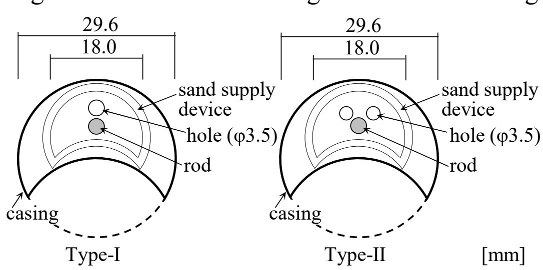

Fig. 4 Schematic of casing and sand supply device

respectively.

The test cases are shown in Table 2. In the three cases, the density of the backfilled sand is varied: loose sand (ML), medium sand (MM), and dense sand (MD). The hardness of the backfill soil was considered by adjusting the filling sand to a predetermined relative density.

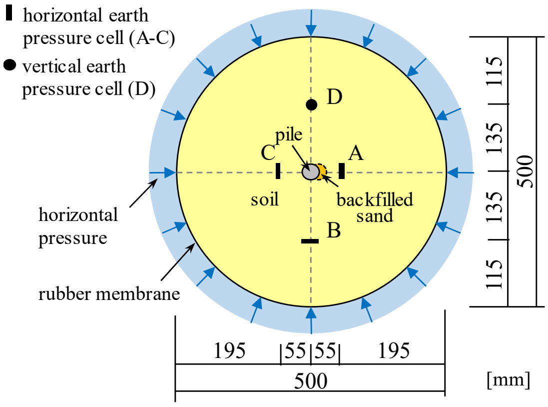

Fig. 5 Layout of earth pressure cell

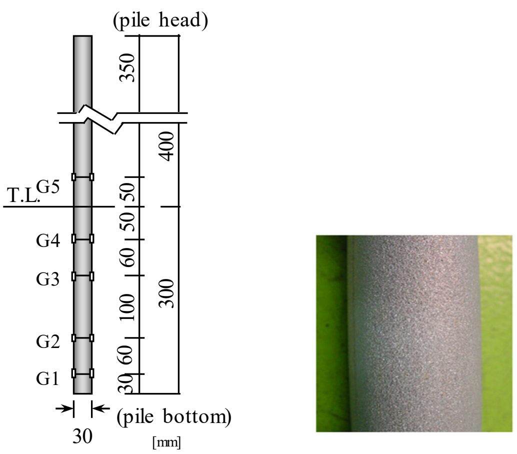

(a) Strain gauge locations (b) Thermal sprayed

Fig. 6 Model pile

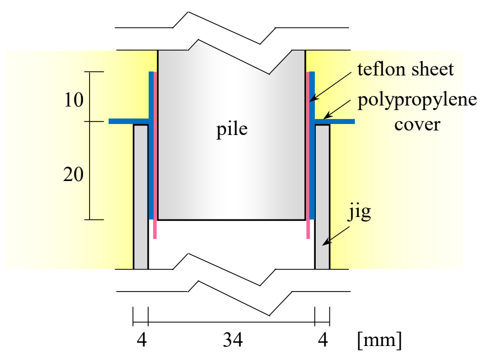

Fig. 7 Layout of pile tip and jig

Table 2 Test cases

		ML	MM	MD
soil	relative density, D_r (%)	60	60	60
backfilled sand	relative density, D_r (%)	30	60	80
	internal friction angle, φ (deg)	29.3	32.1	34.9

2.2 Results and Considerations

Fig. 8 shows the relationship between the shaft resistance of the pile f_s and the displacement at the pile head S_0. The relationship shows a displacement up to 5% (= 1.5 mm) of the pile diameter. f_s is calculated by dividing the axial force difference between the pile head (T.L. in Fig. 6) and the pile tip (G1 in Fig. 6) by the pile circumference area in that section. The axial force was determined based on a calibration test of the model pile that correlated the axial force and the value measured by the specific strain gauge. f_s reached a maximum value at about 0.8 to 1 mm and then decreased to a nearly constant value or a slight decrease to show a residual value. The influence of the relative density of the backfilled sand on the variation of f_s with S_0 is apparent. The maximum value of f_s implies the fully mobilized maximum stresses of the pile shaft resistance. Comparing the maximum value of f_s based on the relative density of backfilled sand, ML and MD are 0.98 times and 1.15 times that of MM, respectively.

The theoretical expression for the maximum pile shaft resistance in sandy soil is as follows:

$$f_s=\sigma_{hf}\cdot\tan\delta=K\cdot\sigma_{v0}\cdot\tan\varphi=\beta\cdot\sigma_{v0} \tag{1}$$

where σ_{hf} is the horizontal stress at failure, σ_{v0} is the initial vertical stress of the soil, and K ($=\sigma_{hf}/\sigma_{v0}$) is a coefficient of horizontal earth pressure.

The third form of the expression in Eq. (1) is known as the β method and is convenient in pile design for estimating shaft resistance [14, 15]. For these tests, β was 0.71 to 0.83.

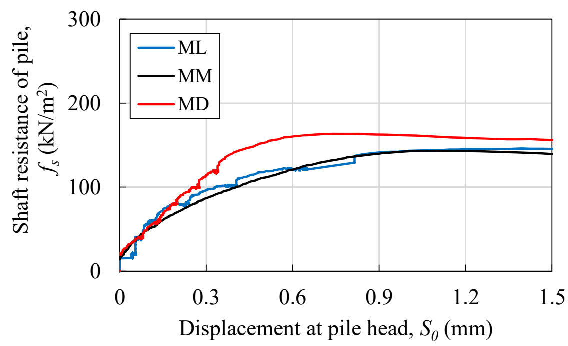

Fig. 8 Shaft resistance of pile

Fig. 9 shows the relationship between the horizontal earth pressures σ_h and the displacement at the pile head. σ_h shows the measured values at the earth pressure cells A and C (in Fig. 5) at the central depth of the pile embedment (T.L. -160 mm). σ_h increases until f_s reaches a maximum. Changes in horizontal stress arise from changes in the volume of the thin shear zone adjacent to the pile shaft [17]. The trend of the change is an increase with increasing level of confinement provided by the surrounding soil [18]. Focusing on the difference depending on the position of the earth pressure cell, in cell-A placed on the backfilled sand side, the earth pressure is smaller when the backfilled sand is loose sand (ML) than for medium density sand (MM), and the earth pressure reaches 1.5 times the horizontal pressure when the backfilled sand is dense sand (MD). It can be inferred that the magnitude of the horizontal stress in the soil increases due to dilation under shear deformation caused by the pushing of the piles. In cell-C on the opposite side, the difference in earth pressure due to the conditions of the backfilled sand is small.

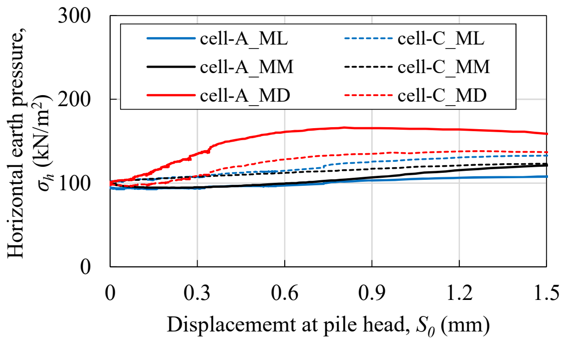

Fig. 9 Horizontal earth pressure (T.L. –160 mm)

3. SIMULATION OF LOADING TEST BY FINITE ELEMENT METHOD

3.1 Analytical Model

The simulation of the loading test was assessed analytically using the SoilPlus FEM software in a three-dimensional model. A representation of the analysis model is shown in Fig. 10, including pile, soil, and backfilled sand. The mesh models half of the geometry considering the boundary conditions of the model. The pile was modeled as a shell element. The soil and backfilled sand were modeled as solid elements. The jig installed at the tip of the pile was expressed by deleting the soil elements in the range corresponding to the jig tip and restraining the side surface of the jig by horizontal displacement.

Tables 3 and 4 show the physical characteristics of the soil, backfilled sand, and pile. The physical properties of the soil and backfilled sand were determined based on soil tests. The pile was considered to be elastic, and the Mohr–Coulomb failure criterion [19, 20] was applied to the soil and backfilled sand.

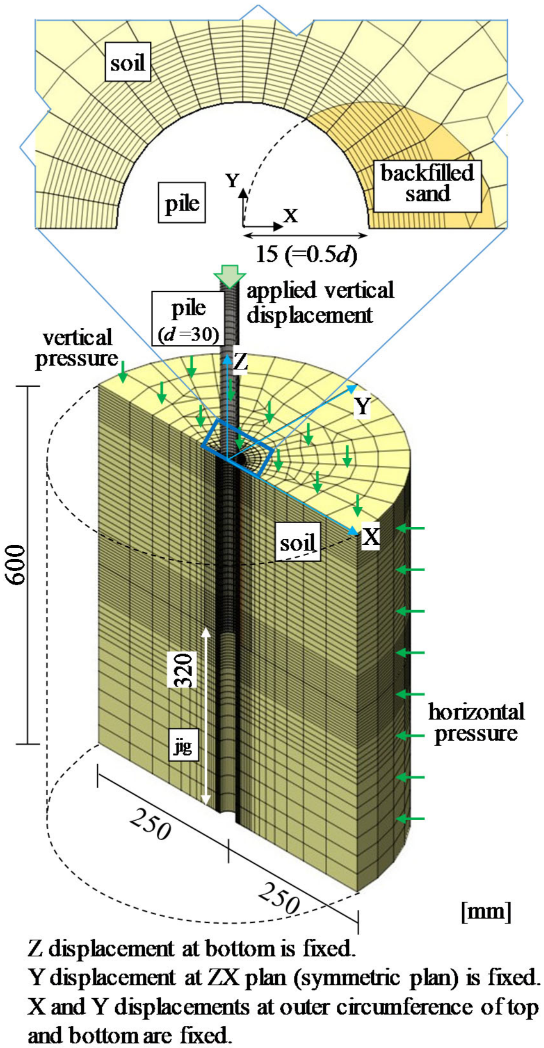

Fig. 10 FEM model

Table 3 Analytical parameters (soil, backfilled sand)

	L	M*	D
Young's modulus, E_s (N/mm^2)		2.72×10^2	
Poison's ratio, ν_s		0.3	
relative density, D_r (%)	30	60	80
density, ρ_s (g/cm^3)	1.49	1.59	1.65
cohesion, c (N/mm^2)		0.01	
internal friction angle, φ (deg.)	29.3	32.1	34.9
dilatancy angle, ψ (deg.)	0.0	2.1	4.9
coefficient, e (= (3 –sinφ)/(3 +sinφ))	0.720	0.699	0.680

*parameter of soil

Table 4 Analytical parameters (pile)

Young's modulus, E_p (N/mm^2)	7×10^4
Poison's ratio, ν_p	0.3
density, ρ_p (g/cm^3)	2.70

After performing an analysis in which a restraining pressure was applied to the side and top surfaces of the soil, an elastoplastic analysis was performed in which the indentation displacement was gradually increased on the pile head. Since the strain-softening of sand cannot be considered in this analysis, a displacement up to 1 mm, which showed the maximum shaft resistance of the pile in the experiment, was examined.

3.2 Comparisons between FEM and Loading Test

The applicability of the analysis model was confirmed by comparing the experimental values (Exp) and analysis values (Ana) for ML and MD.

Figure 11 shows a comparison of the relationship between the shaft resistance of the pile and the displacement at the pile head. The analysis value shows non-linearity of f_s as S_0 increases, similar to the experimental value.

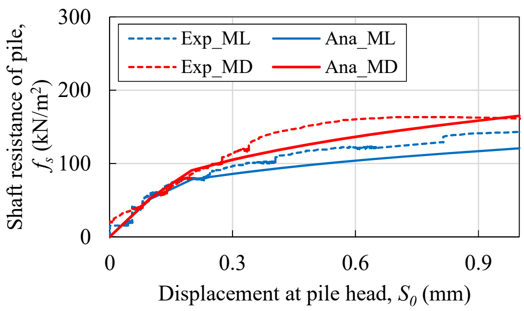

Fig. 11 Relationship between shaft resistances of pile and displacement at the pile head

Figure 12 shows a comparison of the axial force distribution of piles, including the values when the shaft resistance of the pile is maximum and 75% of that in the experiment. The analytical value of the axial force gradually decreases from the pile head in the depth direction and becomes almost 0 at the pile tip, which corresponds to the experimental value over the entire pile length.

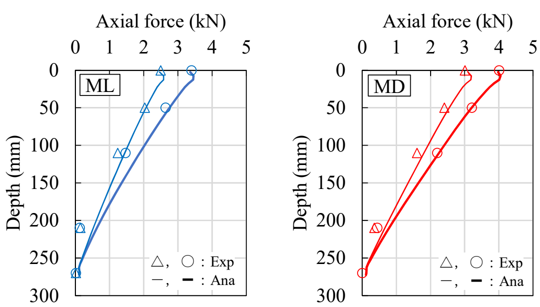

Fig. 12 Axial force distribution of pile

Fig. 13 shows the X-direction distribution of the horizontal earth pressure at the central depth of pile embedment and compares the values when the shaft resistance of the pile was a maximum in the experiment. The analysis value was underestimated compared to the experimental value by 0 to 22%, but the earth pressure tended to increase in the soil near the pile as in the experiment.

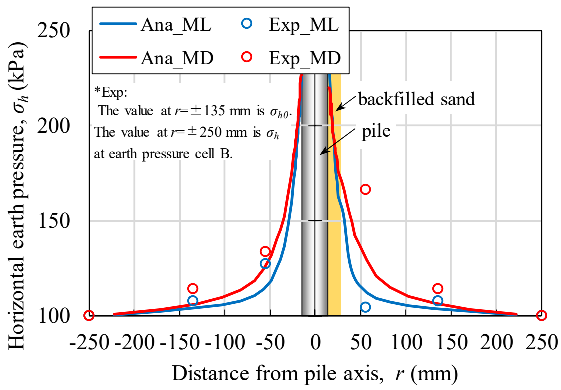

Fig. 13 Comparison of horizontal earth pressure at $Z = -160$ mm between experimental and analytical results

3.3 Considerations for the Shear Failure of the Soil near The Pile

As detailed above, the FEM analysis model could almost reproduce the loading test. In this section, based on the results of the FEM analysis, we consider the deformation, stress, and shear failure that occur in the soil near the pile when the displacement of the pile head S_0 reaches 1 mm (i.e. the shaft resistance of the pile reaches a maximum). The depth of the soil for these results is the central depth of the pile embedment where the typical variations of the shaft resistance of the pile occur.

Fig. 14 shows the downward and horizontal displacement of the soil near the pile. The downward displacement of the soil was greatly deformed locally in the range of 0 to 6 mm from the pile surface, whereas the more distant soil remains largely undeformed. In this test, the surface of the pile shaft is rough. Hence, it is presumed that interlocking of the pile shaft with the soil is such that shearing takes place within a thin shear zone of the soil (i.e. a shear band) immediately adjacent to the loaded pile shaft wall, and not between the sand particles and the pile shaft surface. The vertical displacement is larger on the side where the density of the backfilled sand is higher, and the shear deformation and fracture are different. On the other hand, the horizontal displacement of the soil is largest around 3 mm from the initial offset pile surface and then decays slowly with distance. If the conditions of the backfill sand are different from that of the surrounding soil, the horizontal displacement in the zone adjacent to the pile shaft moves to the low density side.

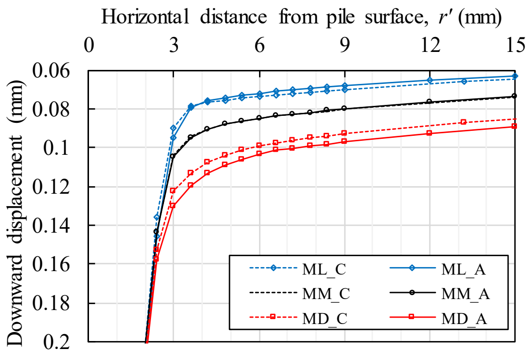

(a) Downward displacement

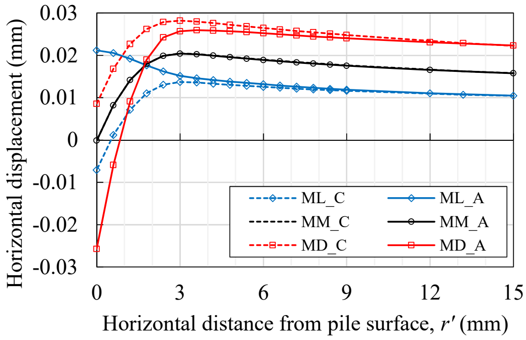

(b) Horizontal displacement

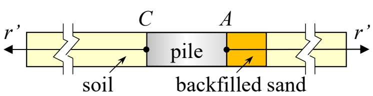

Fig. 14 Downward and horizontal displacement in soil (S_0 = 1 mm, Z = –160 mm)

Next, we consider the shear failure and the shear band that occurs in the soil near the pile. Based on the Mohr–Coulomb failure criterion, the elements of the soil that experienced failure near the pile were determined. The thickness of the shear band was calculated from the distance from the surface of the pile shaft to the failure element of the soil.

Figure 15 shows the shape of the shear band based on the FEM analysis results. The shape is cylindrical for MM. When the backfilled sand overlaps, in the case of ML where the backfilled sand is loose sand, the thickness of the shear band becomes small, but the shape is almost cylindrical. In the case of MD, where the backfilled sand is dense sand, a distorted shape was obtained in which the thickness of the shear band became large, especially in the backfill sand.

Figure 16 shows the thickness α of the shear band. The thickness is 3.2 mm (= 10.1D_{50}) for MM, 2.6 mm (= 8.2 D_{50}) for the thinnest part of ML, and 5.0 mm (= 15.8 D_{50}) for the thickest part of MD. These values are larger than the research results (α= 3–4 D_{50}) by Uesugi et al.[10] focusing on the friction between steel and sand using a friction testing apparatus. It is close to the research results (α= 10–15 D_{50}) by Nemat-Nasser et al.[12], which used a triaxial torsion apparatus.

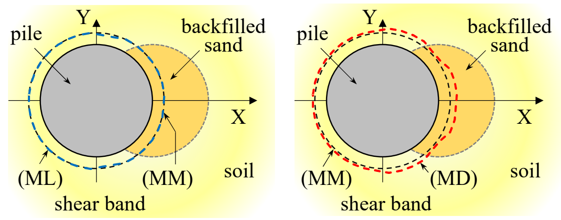

(a) ML (b) MD

Fig. 15 Shape of shear band based on FEM results

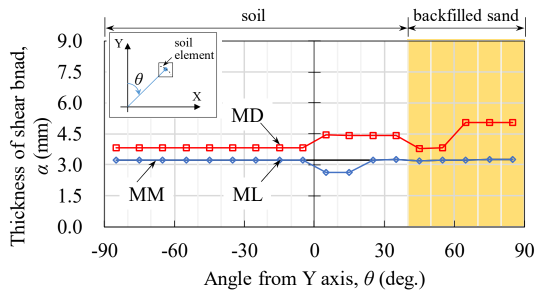

Fig. 16 Thickness of shear band

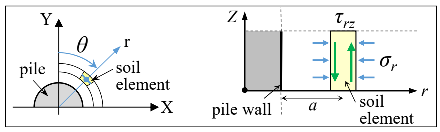

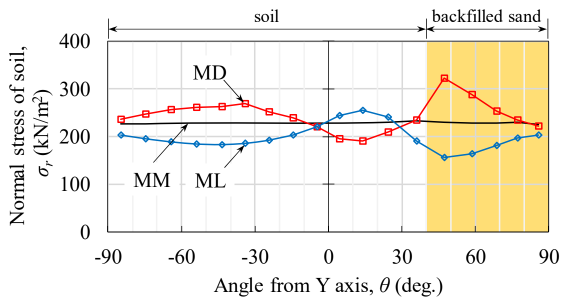

(a) Normal stress, σ_r

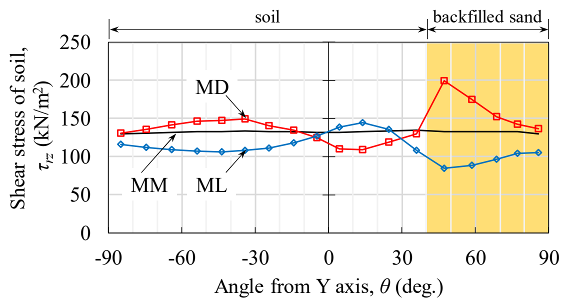

(b) Shear stress, τ_{rz}

Fig. 17 Normal stress σ_r and shear stress τ_{rz} of soil near the pile

Figure 17 shows the normal stress and shear stress (σ_r, τ_{rz}) of the soil on a plane orthogonal to the radial axis at the soil element at the location shown in Fig. 16. The effect of the relative density of the backfilled sand on normal stress and shear stress occurs not only in the area of the backfilled sand but also in the soil on the opposite side. It can be said that an effect of the volume change of sand due to ψ has occurred. The normal stress became about 2.3 times higher for ML, about 1.6 to 2.6 times higher for MM and about 1.9 to 3.2 times higher for MD than the horizontal restraining pressure σ_{h0}.

Finally, the applicability of the case where the shaft resistance of the pile is evaluated using the calculation methods shown in Eqs. (2) and (3) will be examined. In this calculation method, it is considered that the shaft resistance of the pile is expressed by the shear stress of the soil near the pile. The internal friction angle was considered as shown in Eq. (3), because the mode of deformation is not strictly that of simple shear, as the change in soil volume leads to both radial and hoop strains.

$$f_{s,cal}=\sum_{i}\left(\bar{\sigma}_{r,i}\cdot tan\varphi_i'\cdot\frac{d+2\bar{a_i}}{d}\cdot\eta_i\right) \quad (2)$$

$$\varphi_i' = 0.9\varphi_i \quad (3)$$

where $\bar{\sigma}_{r,i}$ is the average value of the normal stress shown in Fig. 17(a) according to the soil density condition, $\bar{a_i}$ is the average value of the shear band thickness shown in Fig. 16 according to the soil density condition, η_i is the ratio of the fracture area for each soil density condition and i is the index of soil density.

Fig. 18 shows a comparison of the pile shaft resistance between the experiment values $f_{s,exp}$ and the calculation values $f_{s,cal}$. The calculation method provides a reasonable agreement with the results from the loading test.

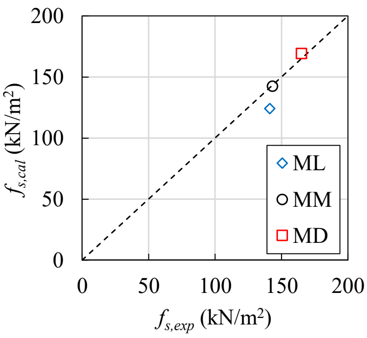

Fig. 18 Comparison of the pile shaft resistance between experiment values $f_{s,exp}$ and calculation values $f_{s,cal}$

The results of the experiments and numerical analysis show that it is necessary to design the shaft resistance of the pile in consideration of the shear band and soil fracture according to the soil conditions around the pile.

It is noted that this study has only investigated the effect of the density of backfilled sand columns. To extend the study, other arrangement and scale of backfilled columns should be considered in the future. Besides, a method will be required to evaluate the change in horizontal stress due to radial displacement caused by sand expansion and the thickness of the shear band based on the physical and mechanical conditions of the soil around the pile, including the backfilled column.

4. CONCLUSIONS

This study investigated the shaft resistance of piles close to backfilled sand. The findings obtained are summarized below.

(1) The maximum shaft resistance of the pile differs depending on the condition of the backfilled sand. The shaft resistance for high density backfilling sand was about 1.15 times that without backfilling sand.

(2) When the conditions of the backfilled sand were different from those of the soil, the shear stress of the soil near the pile was affected not only in the backfilled sand area but also in the soil on the opposite side of the backfilled sand.

(3) When the conditions of the backfilled sand were different from those of the soil, it was considered that the shape and thickness of the shear band near the pile changed.

5. ACKNOWLEDGEMENTS

The author wishes to express gratitude to the members of the research group at the Muroran Institute of Technology for gathering the data for this paper. This work was supported by JSPS KAKENHI Grant Number JP18K04421.

6. REFERENCES

[1] Butcher A.P., Powell J.J.M. and Skinner H.D., Reuse of Foundations for Urban Sites -A Best Practice Handbook-, 2006.

[2] Chapman T., Anderson S. and Windle J., Reuse of foundations, 2007.

[3] Tsubakihara Y. and Yamashita K., Reuse of existing piles in building reconstruction and its environmental effects, The 2005 World Sustainable Building Conference, 2005, pp. 2675-2682.

[4] John H.D.ST. and Chow F.C., Reusing piled foundations -two studies. Reuse of Foundations for Urban Sites-, -Proceedings of the International Conference-, 2006, pp. 357-374.

[5] Patel D., Glover S., Chew J. and Austin J., The Pinnacle Tower – Geotechnical Challenges, International Society for Soil Mechanics and Geotechnical Engineering, Vol. 4, Issue 1,

2010, pp. 9-24.
[6] Watanabe T., Ishizaki S., Tomita N., Kawamoto S. and Tatsuno S., Reuse of existing bored piles for high-rise building foundation, The 15th Asian Regional Conference on Soil Mechanics and Geotechnical Engineering, 2015, pp. 158-161.
[7] Agrawal A., Jalinoos F., Davis N., Hooman E. and Sanayei M., Foundation Reuse for Highway Bridges, FHWA-HIF-18-055 - Report, 2018.
[8] Davis N.T., Hoomaan E., Agrawal A.K., Sanayei M. and Jalinoos F., Foundation Reuse in Accelerated Bridge Construction, Journal of Bridge Engineering,Vol. 24, Issue 10, 2019, Article numbers: 0001455.
[9] Xie J., Gao B. and Chen G., Research on the Construction Technology for the Reconstruction of Existing Retaining Piles under the Condition of the New and Old Foundation Pits in Close Proximity. The 7th International Conference on Environmental Science and Civil Engineering, IOP Conf. Series: Earth and Environmental Science, 719, 2021, Article numbers: 032019.
[10] Uesugi M., Kishida H. and Tsubakihara Y., Behavior of sand particles in sand-steel friction, Soils and Foundations, Vo. 28, Issue 1, 1988, pp. 107-118.
[11] Uesugi M., Kishida H. and Uchikawa Y., Friction between dry sand and concrete under monotonic and repeated loading, Soils and Foundations, Vol. 30, Issue 1, 1990, pp. 115-128.
[12] Nemat-Nasser S. and Okada N., Radiographic and microscopic observation of shear bands in granular materials, Géotechnique, Vol. 51, Issue 9, 2001, pp. 753-765.
[13] Lings M.L. and Diets M.S., The peak strength of sand-steel interfaces and the role of dilation, Soils and Foundations, Vol. 45, Issue 6, 2005, pp. 1-14.
[14] Mascarucci Y., Miliziano S. and Mandolini A., A numerical approach to estimate shaft friction of bored piles in sands, Acta Geotechnica, Vol. 9, Issue 3, 2014, pp. 547-560.
[15] Loukidis D. and Salgado R., Analysis of the shaft resistance of non-displacement piles in sand, Géotechnique, Vol. 58, Issue 4, 2008, pp. 283-296.
[16] Peng S.Y., Ng C.W.W. and Zheng G., The dilatant behaviour of sand–pile interface subjected to loading and stress relief, Acta Geotechnica, Vol. 9, Issue 3, 2014, pp. 425-437.
[17] Yu H.S. and Houlsby G.T., Finite Cavity Expansion in Dilatant Soils: Loading Analysis, Géotechnique, Vol. 41, Issue 2, 1991, pp. 173-183.
[18] Lehane B.M. and White D.J., Lateral stress changes and shaft friction for model displacement piles in sand, Canadian Geotechnical Journal, Vol. 42, Issue 4, 2005, pp. 1039-1052.
[19] Menetrey P. and Willam K., Triaxial Failure Criterion for Concrete and its Generalization, ACI Structural Journal, Vol. 92, 1995, pp. 311-318.
[20] Chen W.F. and Han D.J., Plasticity for structural engineers, 2007.